Super paramagnetic iron oxide MRI shows defective Kupffer cell uptake function in non-alcoholic fatty liver disease

Taketoshi Asanuma, Masafumi Ono, Kei Kubota, et al.

Gut 2010 59: 258-266 originally published online November 16, 2009
doi: 10.1136/gut.2009.176651

Super paramagnetic iron oxide MRI shows defective Kupffer cell uptake function in non-alcoholic fatty liver disease

Taketoshi Asanuma,[1,2] Masafumi Ono,[3] Kei Kubota,[4] Akira Hirose,[3] Yoshihiro Hayashi,[5] Toshiji Saibara,[3] Osamu Inanami,[1] Yasuhiro Ogawa,[4] Hideaki Enzan,[5] Saburo Onishi,[3] Mikinori Kuwabara,[1] Jude A Oben[6,7]

► Supplementary figures are published online only at http://gut.bmj.com/content/vol59/issue2

[1]Department of Radiology, Graduate School of Veterinary Medicine, Hokkaido University, Sapporo, Hokkaido, Japan [2]Department of Veterinary Sciences, University of Miyazaki, Miyazaki, Japan [3]Department of Gastroenterology and Hepatology, Kochi Medical School, Nankoku, Kochi, Japan [4]Department of Radiology, Kochi Medical School, Nankoku, Kochi, Japan [5]Department of Pathology, Kochi Medical School, Nankoku, Kochi, Japan [6]Centre for Hepatology, University College London, UK [7]Guy's and St. Thomas' Hospital, London, UK

Correspondence to
Masafumi Ono, Department of Gastroenterology and Hepatology, Kochi Medical School, Nankoku, Kochi 783-8505, Japan; nom@kochi-u.ac.jp

Received 6 January 2009
Accepted 19 October 2009
Published Online First 16 November 2009

ABSTRACT

Background The pathogenesis of non-alcoholic fatty liver disease (NAFLD) is incompletely understood. Kupffer cells (KCs), phagocytic liver-resident macrophages, provide a protective barrier against egress of endotoxin from the portal to the systemic circulation. It is not known if KC phagocytic function is impaired in NAFLD. Super-paramagnetic iron oxide (SPIO) magnetic resonance imaging is a comparative technology dependent on KC phagocytic function.

Objective To evaluate KC uptake function, in patients and experimental animals with NAFLD, using SPIO.

Methods Abdominal CT and histological examination of liver biopsy specimens were used to estimate the degree of steatosis in patients with NAFLD and controls with chronic hepatitis C. SPIO-MRI was then performed in all patients. Normal rats fed a methionine-choline-deficient diet to induce non-alcoholic steatohepatitis (NASH), the more severe stage of NAFLD, and obese, insulin resistant, Zucker *fa/fa* rats with steatohepatitis, were also studied with SPIO-MRI and analysed for hepatic uptake of fluorescent microbeads. Immunohistochemical analysis evaluated the numbers of KCs in patients and rat livers.

Results Relative signal enhancement (RSE), inversely proportional to KC function, was higher in patients with NAFLD than in controls and with the degree of steatosis on CT. RSE also positively correlated with the degree of steatosis on histology and was similarly higher in rats with induced severe NAFLD (NASH). On immunohistochemistry, defective phagocytic function was the result of reduced phagocytic uptake and not due to reduced KC numbers in rats or patients with NAFLD.

Conclusions KC uptake function is significantly impaired in patients with NAFLD and experimental animals with NASH, worsens with the degree of steatosis and is not due to a reduction of KC numbers.

Non-alcoholic fatty liver disease (NAFLD), is now the most common cause of chronic liver disease in industrialised nations.[1 2] It may progress to cirrhosis.[3] The pathogenesis of NAFLD is incompletely understood but may involve hyper-endotoxaemia, and indeed obesity and type 2 diabetes, commonly present in NAFLD, are associated with endotoxaemia.[4] It was also recently reported that serum endotoxin levels were elevated, compared with controls, in mice fed a methionine-choline-deficient (MCD) diet to induce non-alcoholic steatohepatitis (NASH)—the more severe stage of NAFLD.[5] In addition, serum endotoxin levels in patients with NAFLD are greater than in patients without liver disease,[6] and others have shown raised serum levels of lipopolysaccharide-binding protein (LBP) in patients with NAFLD and more so in patients with NASH.[7] Finally, LBP mRNA levels in the livers of rats with high-fat diet-induced NASH were elevated compared with controls.[8] As Gao and colleagues[8] concluded in their study, therefore, the mechanism of injury in NAFLD may be related to increased levels of endotoxin. This observed hyper-endotoxaemia might be secondary to reduced clearance of endotoxin in NAFLD, possibly caused by an impaired Kupffer cell (KC) uptake function, at least in animal models of NAFLD,[5 9] resulting in overproduction of, and increased sensitivity to, cytokines such as tumour necrosis factor α and interleukin 1β from KCs.[10 11]

KCs are phagocytic macrophages resident in the liver which provide the predominant protection against the egress of endotoxin from the portal to the systemic circulation.[12] The status of KC uptake function in patients with NAFLD is unknown. This has, in part, been owing to an absence of methods to study this parameter reliably in situ. The introduction, however, of super-paramagnetic iron oxide (SPIO) allows such direct studies.

SPIO is a liver-specific magnetic resonance imaging (MRI) contrast agent for detecting hepatocellular carcinoma (HCC).[13 14] The technique relies on the ability of KCs to take up SPIO particles. Since KCs are absent in HCC, differential uptake of SPIO particles allows radiological separation of normal liver from HCC lesions. Following intravenous SPIO, uptake by KCs leads to reduced signal intensity (SI) on T2 MRI sequences, such that, HCC which have no KCs show a high SI. Conversely, areas with abundant KCs show a low T2 SI. In normal liver, therefore, there is a low T2 SI.[15–17] Since the SI with SPIO depends on uptake by KCs of SPIO contrast, SPIO can serve as a surrogate marker of KC uptake function.

In this study, we used SPIO-MRI to test the hypothesis that patients with NAFLD have impaired KC uptake function. To investigate the underlying mechanisms and ascertain that impaired KC uptake function was not due to a reduction in KC numbers, we then used SPIO along with ingestion of fluorescent microbeads in rats fed an MCD diet as a model of NASH, a severe stage of NAFLD[18 19] and in obese, insulin resistant, steatohepatitic Zucker *fa/fa* rats, as an additional

model of NASH. In addition, immunohistochemical analysis with a KC-specific antibody and computerised-image analysis evaluated the number of KCs in livers of rats fed an MCD diet and in liver biopsy specimens from patients with NAFLD.

Our results show that both in an animal models of severe NAFLD—that is, NASH, and in patients with NAFLD, KC uptake function is impaired. This impairment is not due to a reduction in KC numbers. These findings may explain why there is a hyper-endotoxaemic state in NAFLD and suggest that strategies to enhance KC uptake function and/or reduce endotoxin levels may be of benefit in treating NAFLD.

MATERIALS, PATIENTS AND METHODS

Animals

Six-week-old male Wistar rats were fed either an MCD diet (Oriental Yeast, Tokyo, Japan, n=16) or a normal diet (n=16) for 12 weeks. Obese Zucker *fa/fa* rats (18 weeks old male, n=8) known to have insulin resistance and steatohepatitis served as another model of NASH, with their lean controls. All animal experiments were approved by our local animal use committee.

SPIO contrast agent

Resovist (Nihon Schering, Osaka, Japan) used as the SPIO contrast agent is a hydrophilic colloidal solution of SPIO coated with carboxydextran (γ-Fe_2O_3/$C_6H_{11}O_6$-($C_6H_{10}O_5$) n-$C_6H_{11}O_5$).[20]

Animal MRI

All animal MRI examinations were performed, using a Varian Unity INOVA NMR console coupled to a Sun Microsystems host computer running VNMR 6.1 C software (Varian, Palo

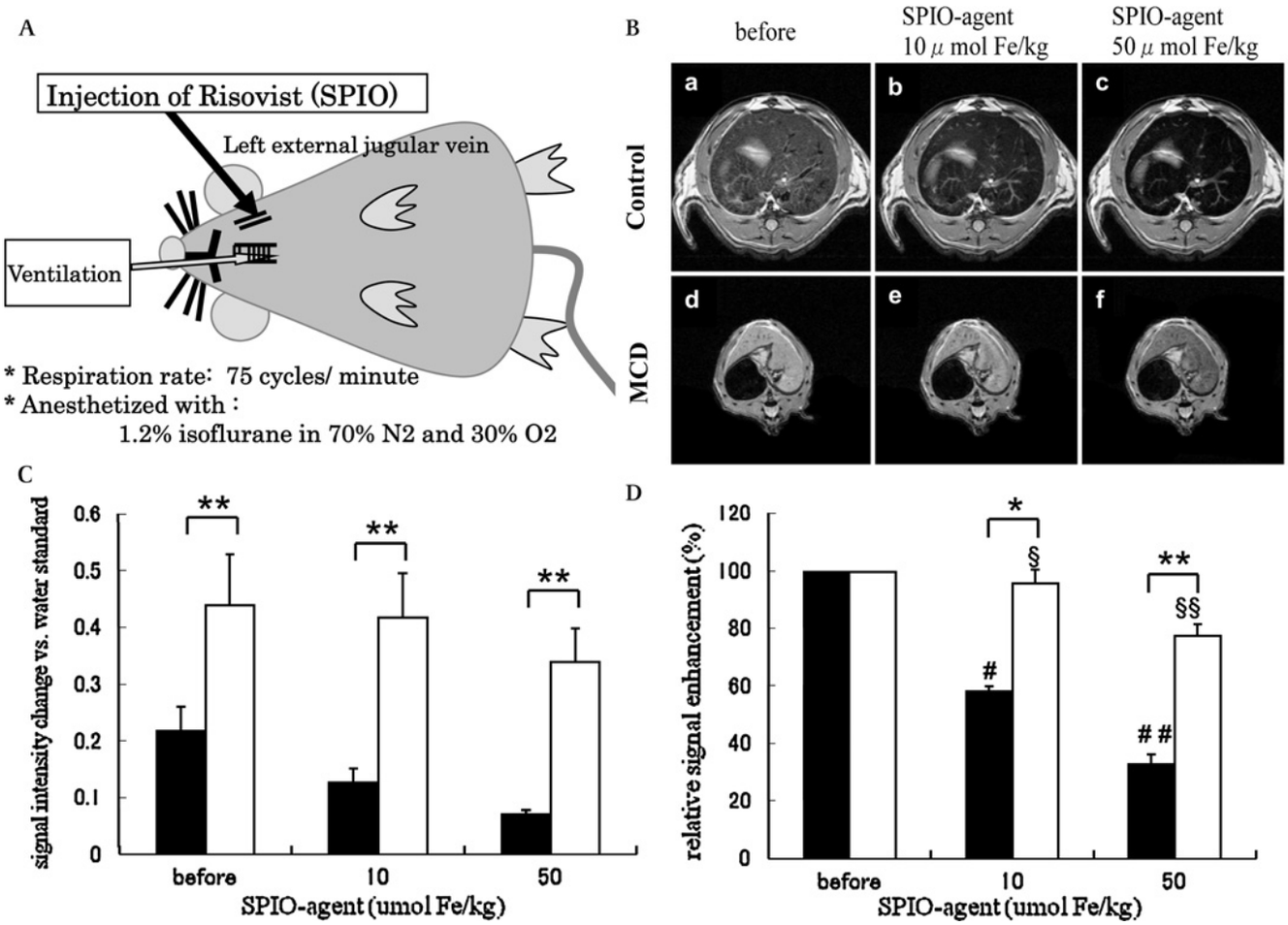

Figure 1 Rat super-paramagnetic iron oxide (SPIO)-MRI studies. (A) Schema of the rats SPIO-MRI experiment. The rats were tracheotomised, intubated and anaesthetised with 1.2% isoflurane in 70% N_2 and 30% O_2 during the MRI experiments. Ventilation rate was adjusted to 75 cycles/min for synchronising with the gating apparatus of the MRI. SPIO contrast was administered via a cannulated left external jugular vein. (B) Representative MR images of rat SPIO studies. After SPIO administration, the signal intensity (SI) of control rats dramatically decreased, whereas little signal reduction was seen in rats fed a methionine-choline deficient (MCD) diet. (C) Changes of SI in rat livers. Signal reduction occurred in control (n=4) and rats fed an MCD diet (n=4), respectively, after injection of SPIO (**$p<0.01$). ■, control rats; □, rats fed an MCD diet. (D) Here, SI was compared as a relative signal enhancement (RSE; %). After infusion of SPIO (10 μmol Fe/kg), a substantial reduction of SI was seen in control rats (RSE=100% vs 58.0±2.0%, #$p<0.05$), whereas there was no statistically significant reduction in RSE in the livers of rats fed an MCD diet (RSE=100% vs 95.4±4.7%, §$p>0.05$). With SPIO at 50 μmol Fe/kg a more marked reduction in RSE, than was seen at 10 μmol Fe/kg, was seen with control rats (100% vs 32.5±3.6%, n=4, ##$p<0.05$) compared with rats fed an MCD diet (100% vs 77.3±3.7%, n=4, §§$p<0.05$). Furthermore, there was a clear and statistically significant difference in RSE between control and rats fed an MCD diet at either of the SPIO concentrations, with the RSE of the rats fed an MCD diet being consistently higher than controls (95.4±4.7% vs 58.0±2.0%, *$p<0.05$ at SPIO 10 μmol Fe/kg, and 77.3±3.7% vs 32.5±3.6%, **$p<0.05$ at SPIO 50 μmol Fe/kg). ■, control rats; □, rats fed an MCD diet.

Alto, California, USA) equipped with a 18.3 cm horizontal-bore 7.05 Tesla superconducting magnet (Oxford Instruments, UK).[21 22] To minimise bulk motion artefacts, data acquisitions were gated to respiration using a home-made mechanical switch activated by the ventilator piston at inspiration. This gating apparatus synchronised the rat respiration and the start of pulse sequence. The rats were anaesthetised, tracheotomised and ventilated with 800 ms/respiration cycle (figure 1A).

MR images were obtained using a spin-echo (SE) sequence. Repetition time (TR) was determined by the respiration rate and the number of multislice, and was 4800 ms (=800 ms×6 slices). Unenhanced MR images of the liver were first obtained, and then MRI was performed 15 min after the injection of SPIO (10 μmol Fe/kg body weight or 50 μmol Fe/kg body weight) via the left external jugular vein.

SI values of the liver parenchyma in the region of interest (over 100 pixels) were normalised to the standard deviation of background noise and expressed as signal-to-noise ratio. SI of the whole liver was measured on each MR image, and the relative signal enhancement (RSE) of the rat liver was calculated using the following equation: RSE (%)=SIpost/SIpre×100, where SIpre and SIpost are the signal intensities of the whole liver parenchyma before and after injection of SPIO respectively.[16]

Evaluation of accumulation of fluorescent microspheric beads in rat livers

Rats fed an MCD diet (n=6) and control rats (n=6) or Zucker *fa/fa* rats (n=4) were deeply anaesthetised with pentobarbital sodium (25–50 mg/kg, Nembutal; Abbott Laboratories) administered intraperitoneally, and Fluoresbrite YG carboxylate microspheres 2.00 μm (2.5% slide-latex, Polyscience, Warrington, Pennsylvania, USA) were injected via a left external jugular vein catheter. One hour after injection, the animals were re-anaesthetised, and their livers removed. The number of accumulated microspheres in 10 high-power fields was counted by fluorescent microscopy.

Kupffer cells in liver sections

Liver sections were stained for the presence of KCs with ED2 monoclonal antibody (BMA Biomedicals AG, Switzerland).[23] The number of KCs per field area of digital photomicrographs was quantified with a computerised image analysis system (Macintosh MacSCOPE version 2.591).[18]

Patients

Twenty-six patients (14 women/12 men) with elevated transaminases and a diagnosis of NAFLD on abdominal ultrasonography, and 10 patients with chronic hepatitis C (five women/five men) and four healthy volunteers as controls, participated in this study. Patients with known use of methotrexate, tamoxifen, corticoids, insulin or alcohol in excess of 20 g per day and patients with other known causes of liver disease, including viral hepatitis, haemochromatosis, Wilson disease and autoimmune liver diseases, were excluded from this study. Informed consent was obtained for SPIO-MRI, abdominal CT, liver biopsy or laboratory tests. Twenty-six patients with NAFLD consented to an abdominal CT scan to quantify the degree of hepatic steatosis, defined as a liver/spleen ratio (L/S ratio): <0.9 moderate to severe hepatic steatosis and ≥0.9 mild hepatic steatosis.[24] Liver biopsies were also performed in 20 patients with NAFLD: 13 (seven women/men men) of these fulfilled criteria diagnostic for NASH.[25]

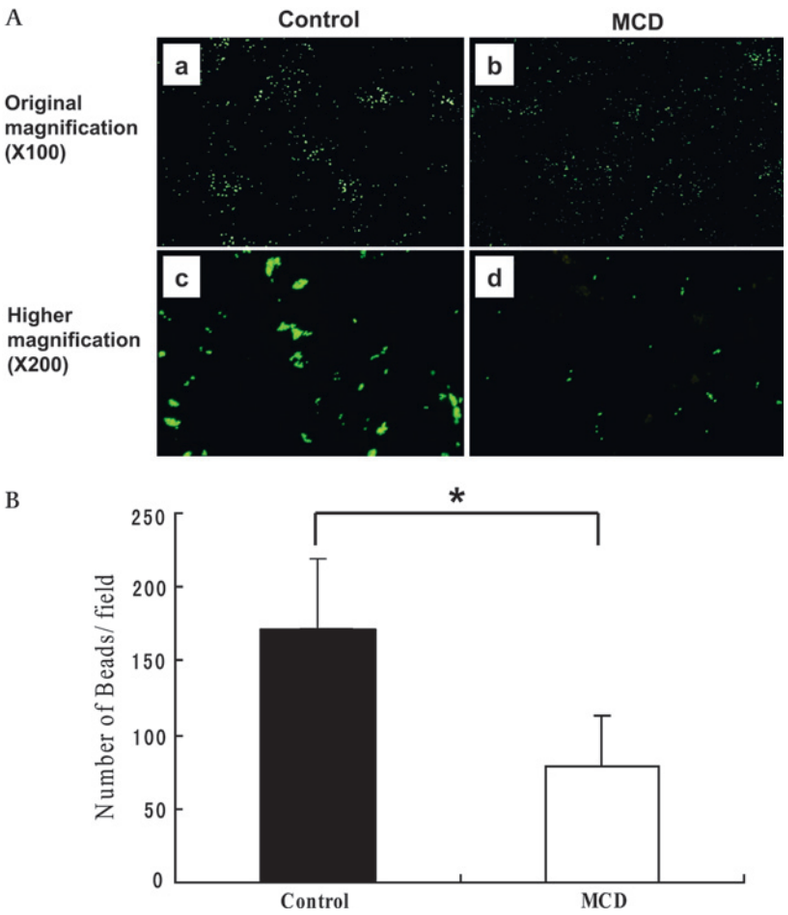

Figure 2 Uptake of fluorescent microspheric beads by Kupffer cells. (A) Uptake of microbeads in a liver section as judged by fluorescent microscopy. Fluorescent microbeads formed large aggregates in control livers, whereas the beads were disseminated in the livers of rats fed a methionine-choline deficient (MCD) diet. (B) The number of fluorescent microbeads taken up in liver sections of control and rats fed an MCD diet. The number of fluorescent beads in livers of rats fed an MCD diet was fewer than that in control rat livers (171.33±48.37/field in control rats (n=6), 78.63±34.8/field in rats fed an MCD diet (n=6), *p<0.005). ■, control rats; □, rats fed an MCD diet.

Patient MRI

MRI examinations were performed on a 1.5 T MRI system (Signa Horizon, GE Medical Systems, USA) using a body phased array coil. Unenhanced T1- and T2-weighted images of the whole liver were obtained as routine. SPIO (8 μmol Fe/kg body weight) was injected via the antecubital vein. Fast imaging was performed using the SPGR (spoiled gradient recalled acquisition in the steady state) technique at 200/20/20 degree (TR/TE/flip angle) in suspended respiration to analyse the uptake of SPIO by the liver. Whole-liver images were acquired within 15 s.

The parameters used were field of view, 320×320 mm; slice thickness, 7.0 mm; interslice gap, 3.0 mm, phase×frequency matrix, 128×256; and number of acquisitions, one. SPGR imaging was repeated at multiple time points (pre-contrast, 40 s, 2, 3, 5, 10, 15, 20, 25 and 30 min after injection of SPIO). The RSE was calculated as above.

Histological examination

Haematoxylin and eosin stained liver biopsy specimens of patients with NAFLD were scored according to the NASH Clinical Research Network Scoring System[24] by two pathologists blinded to the patients' clinical data. An NAFLD Activity Score (NAS) of ≥5 was classified as NASH and ≥3 as non-NASH.[25]

KCs in patients' liver biopsy specimens

KCs in liver biopsy specimens were detected by staining with anti-CD68 (KP-1, DAKO)[18] and quantified as above.[18]

Statistical analysis

Results are presented as mean±SD for continuous data or as numbers for categorical data. A univariate analysis was conducted using the Mann–Whitney U test to assess the significance between the two groups based on the quantitative data. Qualitative data were compared using Fisher's exact test. Spearman's coefficient of correlation was used to evaluate the relationship between the two groups. Statistical significance was accepted at $p<0.05$. All analyses were performed using Stat View.

RESULTS

Rats with experimentally induced NASH have reduced KC uptake function

Figure 1B shows representative MR images of rats fed a control or MCD diet with and without infusion of SPIO. Images were scarcely affected by motion artefact (a). In the absence of SPIO, livers of rats fed an MCD diet (d) had a higher SI than control rats (a). After SPIO (10 μmol Fe/kg), SI in control livers dramatically decreased (b), whereas little signal reduction was seen in livers of rats fed an MCD diet (e). Similarly, after 50 μmol Fe/kg SPIO, the SI of the control livers almost disappeared (c), with minimal signal reduction in MCD-fed rats (f).

Figure 1C shows quantitatively the changes in SI in control or MCD-fed rats, depicted qualitatively in figure 1B above. Signal intensities were standardised using the SI of water as an external standard. At baseline there was a statistically significant difference between the SI of control and MCD-fed rats (0.22±0.04 vs 0.44±0.09, $p<0.01$). After infusion of 10 and 50 μmol Fe/kg

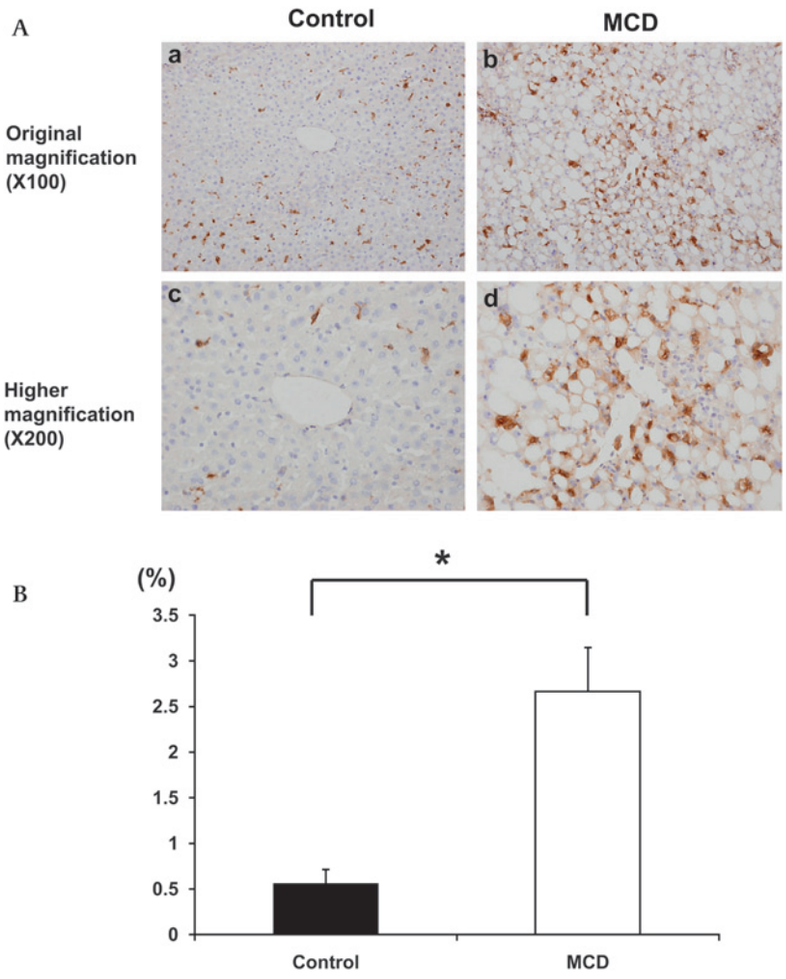

Figure 3 The number of Kupffer cells (KCs) in the livers of rats fed a methionine-choline deficient (MCD) diet. (A) Immunostaining of KCs in liver sections. The number of KCs in the livers of rats fed an MCD diet was increased compared with that of controls. (B) The area occupied by KCs cells estimated by image analysis in the livers of rats fed an MCD diet (2.6675±0.4795%, n=6) is clearly shown to be increased compared with that of control rats (0.5606±0.1541%, n=6, *$p<0.0001$). ■, control rats; □, rats fed an MCD diet.

SPIO, this difference was accentuated and a greater SI reduction was seen in controls than in MCD-fed rats (0.13±0.03 vs 0.42±0.08 at 10 μmol Fe/kg SPIO and 0.069±0.009 vs 0.337±0.063 at 50 μmol Fe/kg SPIO, p<0.01), with minimal change of SI in the MCD-fed at each SPIO dose.

To more accurately compare the uptake function of KCs observed with an MCD diet, SIs were calculated as the RSE (figure 1D), with the RSE at baseline set at 100%. After infusion of SPIO (10 μmol Fe/kg), a substantial reduction of SI was observed in controls (RSE=100% vs 58.0±2.0%, p<0.05), whereas there was no significant reduction in RSE in rats fed an MCD diet (RSE=100% versus 95.4±4.7%, p>0.05). With infusion of SPIO at 50 μmol Fe/kg a more marked reduction in RSE, than was seen at 10 μmol Fe/kg, was found with controls (100% vs 32.5±3.6%, p<0.05) compared with rats fed an MCD diet (100% vs 77.3±3.7%, p<0.05). Furthermore, there was a clear and statistically significant difference (p<0.05) in RSE between control rats and rats fed an MCD diet at either of the SPIO concentrations, with the RSE of the rats fed an MCD diet being consistently higher than controls (95.4±4.7% vs 58.0±2.0%) at SPIO 10 μmol Fe/kg, and (77.3±3.7% vs 32.5±3.6%) at SPIO 50 μmol Fe/kg. Therefore, uptake function of KCs in rats fed an MCD diet is impaired compared with that in control rats.

Similarly, as shown in online supplementary figure 1, the RSE of SPIO-MRI in Zucker *fa/fa* rats was significantly higher than that of their lean littermates (59.5±12.5% vs 47.2±11.7% at SPIO 10 μmol Fe/kg, p<0.05, and 27.0±9.8% vs 18.2±9.0% at SPIO 50 μmol Fe/kg, p<0.05) indicating that KC uptake function in the livers of obese, insulin-resistant, steatotic Zucker *fa/fa* is impaired compared with that of controls and so validating the results with the rats fed an MCD diet as above.

Uptake of fluorescent beads by KCs is reduced in experimental NASH

To confirm this suggested impairment of KC uptake function in our experimental models of NASH, fluorescent microspheric beads were now infused into the rats fed an MCD diet and Zucker *fa/fa* rats and the number of fluorescent beads in their livers enumerated to reflect clearance function of KCs.[13] Qualitatively, figure 2A shows that the fluorescent microspheric beads in the livers of rats fed an MCD diet were fewer (figure 2A, b and d) than in controls (figure 2A, a and c). Furthermore, the beads formed large aggregates in control livers (figure 2A, a and c), whereas they were disseminated in the MCD-fed rats liver (figure 2A, b and d). Quantitatively, there were fewer fluorescent beads in the livers of rats fed an MCD diet than in controls (171.33±48.37/field (n=6), controls vs 78.63±34.8/field (n=6), rats fed an MCD diet, p=0.003, figure 2B).

We also examined the correlation between the extent of hepatic steatosis and KC uptake function, and between NASH activity and KC uptake function in MCD-fed rats. Online supplementary figure 2 shows that the number of phagocytosed microbeads in the livers of rats fed an MCD diet after 12 weeks (78.63±34.81/field) was no different from that after 4 weeks of the MCD diet (75.15±6.69/field, p=0.873). The extent of steatosis was similar between rats at 12 weeks and 4 weeks, although the extent of hepatic fibrosis and inflammation were more severe at 12 weeks than at 4 weeks. Furthermore, the number of microbeads taken up after 2 weeks of the MCD diet (non-NASH with mild steatosis, 131.02±22.75/field) was higher than that at 4 weeks (severe hepatic steatosis, 75.15±6.69/field, p<0.01). These data suggests that KC uptake function in rats is not influenced by NASH activity or severity but rather by the extent of hepatic steatosis.

As with the rats fed an MCD diet, accumulation of fluorescent microbeads in the livers of steatotic Zucker *fa/fa* rats (online supplementary figure 3A) was significantly lower than that of their lean littermates (173.94±10.84/field vs 221.01±11.11/field, n=4, p<0.005; online supplementary figure 3B). Thus, the uptake function of KCs is reduced in experimental NASH.

KCs numbers in livers of rats fed an MCD diet are increased compared with controls

We next evaluated the number of KCs in the livers of rats fed an MCD diet by immunohistochemical staining with ED2 monoclonal antibody without infusion of fluorescent beads. The number of KCs in the livers of rats fed an MCD diet was significantly increased compared with control livers (figure 3A, a–d). In addition, the morphological appearance of the KCs was altered and they appear enlarged in the livers of MCD-fed rats (figure 3A, c and d). To quantity the number of KCs, the area occupied by KCs was estimated by image analysis. The area occupied by KCs in the livers of rats fed an MCD diet was clearly increased compared with that of control rats (2.6675±0.4795% (n=6) vs 0.5606±0.1541% (n=6), p<0.0001, figure 3B). Therefore, the impairment of KC uptake function in the MCD model of NAFLD is functional and is not due to a reduction in the numbers of KCs.

SPIO-MRI in patients with NAFLD

KC uptake function is impaired in patients with NAFLD

To determine the applicability of these animal studies to NAFLD, we now evaluated, using SPIO-MRI, the uptake function of KCs in the livers of patients with NAFLD and chronic hepatitis C (CH-C) as controls. The clinical characteristics of the CH-C and NAFLD groups are shown in table 1. Patients with NAFLD were younger and had higher body mass indices, calculated as weight (kg) divided by height (m) squared, than those with CH-C.

Table 1 Comparison of clinical characteristics of patients with chronic hepatitis C (CH-C) and non-alcoholic fatty liver disease (NAFLD)

	CH-C (n=10)	NAFLD (n=26)	p Value
Female/male	5/5	14/12	0.842
Age (years)	61.4±9.88	48.2±17.5	<0.05
BMI (kg/m^2)	22.9±2.7	31.1±6.8	<0.01
RBC (×10^4/μl)	428.0±40.1	464.4±50.3	<0.05
Ht (%)	40.0±3.8	42.6±4.2	0.099
Plt (×10^4/μl)	19.5±8.4	21.2±6.1	0.422
WBC (×10^3/μl)	4.724±1.321	6.260±1.967	<0.05
ALT (U/l)	41.6±22.3	82.2±62.2	0.056
AST (U/l)	40.3±17.4	55±35.0	0.184
LDH (U/l)	185.1±26.0	214.2±54.7	0.124
ALP (U/l)	255.6±88.5	227.9±56.8	0.209
γ-GTP (U/l)	28.1±13.4	60.8±36.2	<0.05
T-Bil (mg/dl)	0.58±0.24	0.84±0.32	<0.05
TP (g/dl)	7.76±0.37	7.39±0.47	<0.05
Alb (g/dl)	4.29±0.13	4.44±0.29	0.089
PT (%)	82.0±9.2	87.5±11.6	0.104
T-cho (mg/dl)	173.4±37.9	192.0±35.4	0.177
TG (mg/dl)	135.3±61.3	160.1±72.6	0.572
FPG (mg/dl)	101.4±11.9	108.8±34.9	0.498

Patients with NAFLD were younger and had higher BMI than those with CH-C (p<0.05). Alb, albumin; ALP, alkaline phosphatase; ALT, alanine transaminase; AST, aspartate aminotransferase; BMI, body mass index; FPG, fasting plasma glucose; Ht, haematocrit; γ-GTP, γ-glutamyltransferase; LDH, lactate dehydrogenase; Plt, platelets; PT, ????; RBC, red blood cells; T-Bil, total bilirubin; T-cho, total cholesterol; TG, triglycerides; TP, ????; WBC, white blood cells.

The liver MRI images before and after SPIO in patients with CH-C or NAFLD are shown in figure 4A. As shown, the SI of the liver images in CH-C decreased within 15 min after injection of SPIO. However, only a slight reduction of SI was seen in livers with NAFLD. We next compared the RSE in patients with CH-C and NAFLD. As shown, figure 4B, RSE in NAFLD was significantly higher than in controls (20.87±6.23% (n=26) vs 10.13±1.31% (n=10), $p<0.0001$), indicating that KC uptake function is impaired in NAFLD. Furthermore, we also studied SPIO-RSE in healthy volunteers (n=4). The RSE of healthy volunteers was almost the same as that of patients with CH-C (online supplementary figure 4B), but was demonstrably lower than that of patients with NAFLD (online supplementary figure 4A, $p=0.0011$).

KC uptake function in NAFLD worsens with the degree of hepatic steatosis

We next evaluated the relationship between RSE and degree of hepatic steatosis determined on abdominal CT. The RSE in patients with NAFLD with mild hepatic steatosis was significantly lower than in patients with moderate to severe hepatic steatosis (16.77±4.44% (n=8) vs 23.77±6.29% (n=14), $p<0.05$, figure 4C). Since the RSE is inversely proportional to KC function—that is, the larger the RSE, the worse the KC function, these results suggest therefore that KC uptake function worsens with the degree of hepatic steatosis in NAFLD.

We now sought to determine if KC uptake function was also related to the degree of steatosis on biopsy. We observed a strong positive correlation between the degree of hepatic steatosis and RSE on SPIO-MRI in the livers of patients with NAFLD (figure 4D, $r=0.757$, $p<0.0005$, n=20), confirming that the degree of KC uptake dysfunction in NAFLD is related to the extent of hepatic steatosis.

We also determined if age might have influenced the RSE on SPIO-MRI in our study. As shown in our online supplementary figure 5A, there was no significant correlation between age and RSE in the CH-C cohort. However, there was a significant correlation between age and RSE in patients with NAFLD

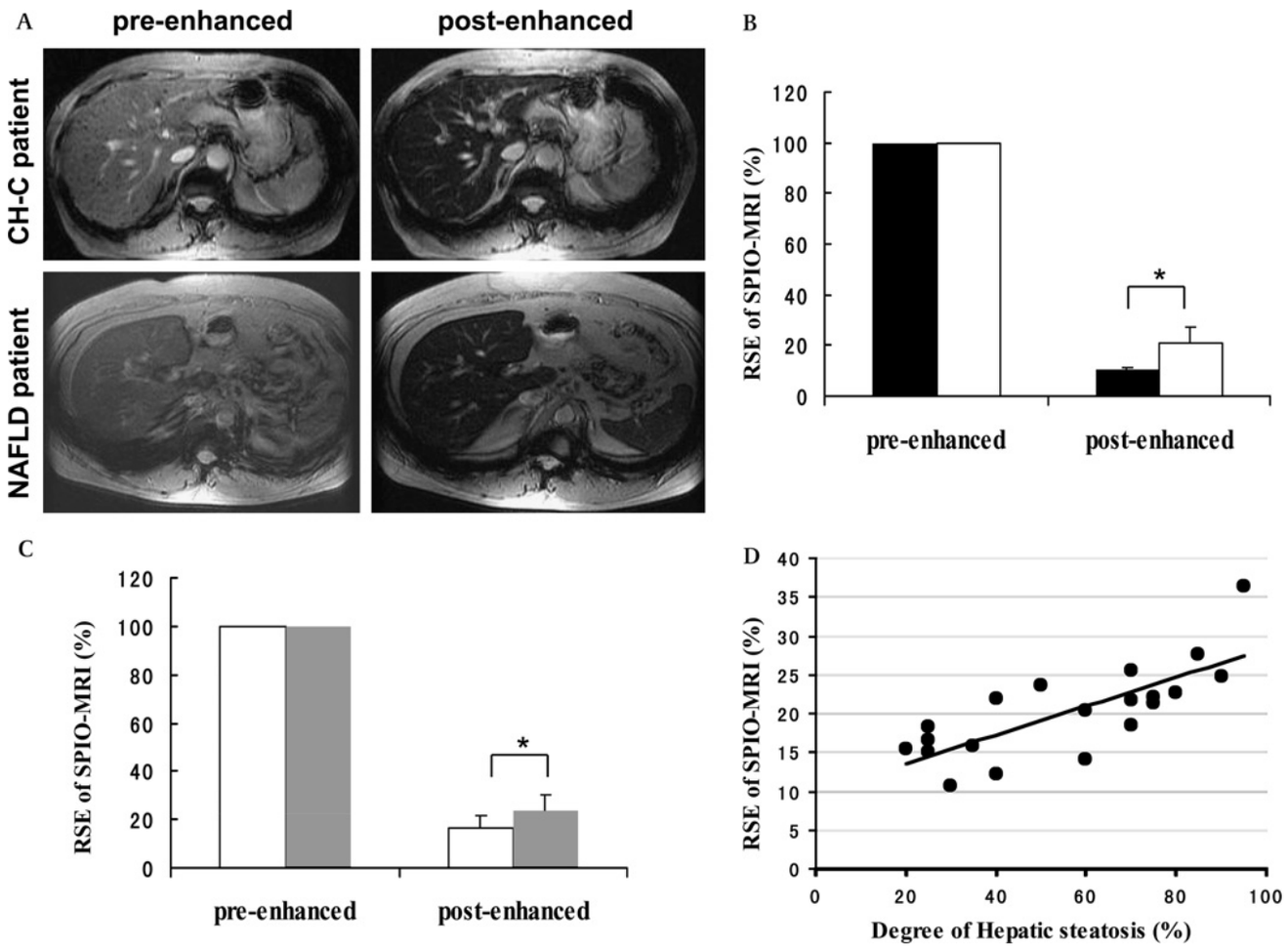

Figure 4 Super-paramagnetic iron oxide (SPIO)-MRI in patients with non-alcoholic fatty liver disease (NAFLD). (A) Representative MRI images of a patient with NAFLD and another with chronic hepatitis C (CH-C), pre-enhancement and post-enhancement with SPIO. (B) The relative signal enhancement (RSE) of the livers of patients with NAFLD and CH-C controls. RSE in the NAFLD group was statistically higher than in the CH-C control group (20.87±6.23% (n=26) vs 10.13±1.31% (n=10), *$p<0.0001$). ■, CH-C; □, NAFLD. (C) Relationship between the RSE and the degree of hepatic steatosis on abdominal CT. The RSE of patients with NAFLD who had mild hepatic steatosis was remarkably lower than that in patients with NAFLD who had moderate to severe hepatic steatosis (16.77±4.44% (n=8) vs 23.77±6.29% (n=14), *$p<0.05$). □, NAFLD with mild hepatic steatosis; ■, NAFLD with moderate to severe hepatic steatosis. (D) Relationship between degree of hepatic steatosis and RSE of SPIO-MRI in patients with NAFLD. A strong positive correlation was observed between the degree of hepatic steatosis and the RSE on SPIO-MRI in the livers of patients with NAFLD ($r=0.757$, $p<0.0005$, n=20).

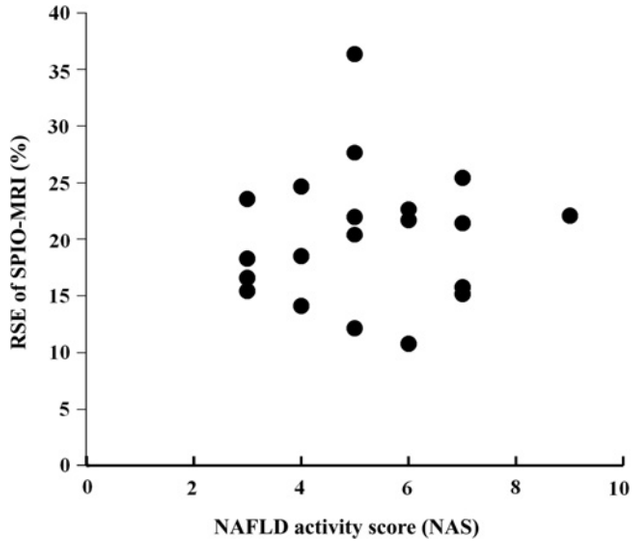

Figure 5 The relationship between non-alcoholic fatty liver disease (NAFLD) activity score (NAS) and relative signal enhancement (RSE) in patients with NAFLD. With NAS, 13 patients out of 20 were diagnosed as having the non-alcoholic steatohepatitis stage of NAFLD. The RSE of super-paramagnetic iron oxide (SPIO)-MRI in the 20 patients with NAFLD was not correlated with NAS (r=0.0682, p=0.8072, n=20).

(online supplementary figure 5B). In addition, the younger patients with NAFLD had more severe hepatic steatosis than the older patients in our study (online supplementary figure 5C). Therefore, RSE in NAFLD patients is influenced not by age but by the degree of hepatic steatosis.

KC uptake function is not related to NAFLD activity score

To now determine the relationship between the severity of NAFLD, as judged by the NAS and RSE, liver biopsies were scored according to the NASH Clinical Research Network Scoring System.[25] Accordingly, 13 of the 20 patients with NAFLD were classified as having NASH. The NAS was then correlated with RSE. As shown in figure 5, there was no correlation between the RSE and NAS, suggesting that KC uptake function may not be related to histological severity of NAFLD.

Reduced KC uptake function in NAFLD is not dependent on a reduction on the number of KCs

As with the rat studies, we now sought to determine if the apparent KC dysfunction in NAFLD was secondary to a lowering of the number of KCs. To this end we stained for the presence of KCs by immunohistochemistry and quantified the numbers by image analysis. There was no correlation ($p>0.05$) between the severity of steatosis and number of KCs, nor between the number of KCs and RSE (figure 6A–C). Therefore, the observed reduction in KC uptake function in NAFLD is not dependent on a reduction in KC numbers.

Reduced KC uptake function in NAFLD is not dependent on reduced hepatic blood flow

It is plausible that the changes in RSE in patients with NAFLD and CH-C were due to changes in the liver's microcirculation since fat accumulation in hepatocytes is associated with increases in hepatocyte cell volume which may compromise the hepatic sinusoidal space.[26] To ensure that changes in RSE in patients with NAFLD and CH-C were not due to changes in microcirculatory blood flow, we therefore compared the change in RSE with, time after injection of SPIO, in both patient groups. RSE gradually decreased in both groups after injection of SPIO and had reached a plateau by 15 min (figure 7). Consequently, differences at 15 min were reasonably chosen as standard in all the human studies above and observed differences between the NAFLD and control groups are unlikely, therefore, to be the result of changes in the microcirculation.

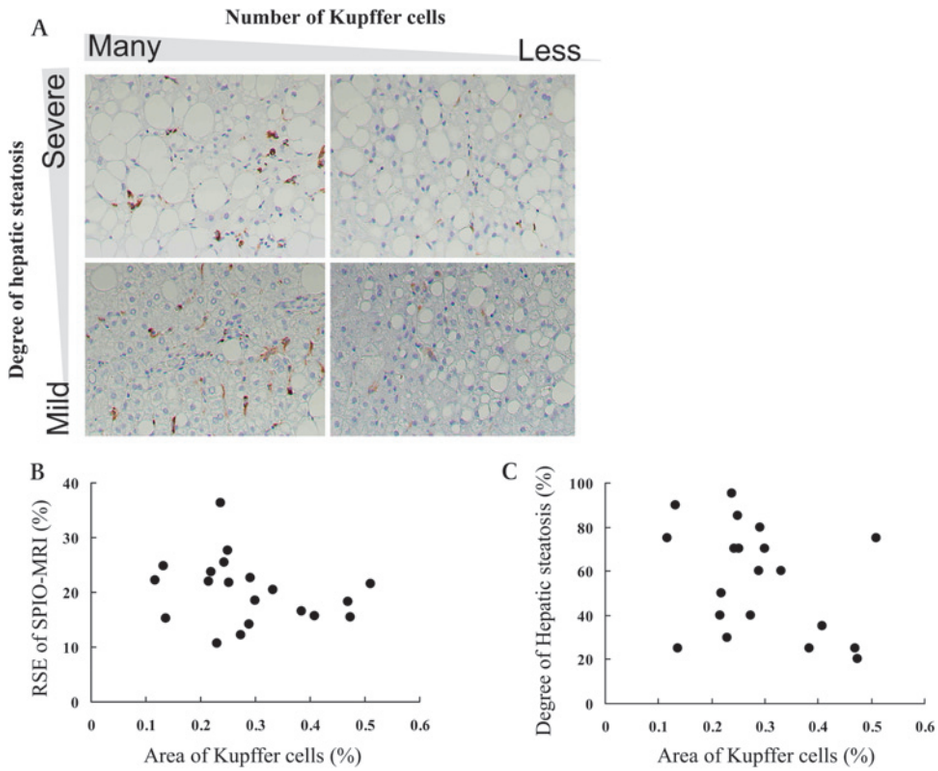

Figure 6 The number of Kupffer cells (KCs), degree of hepatic steatosis and relative signal enhancement (RSE) in patients with non-alcoholic fatty liver disease (NAFLD). (A) Four typical histological patterns based on the degree of fatty droplets and the number of KCs in the liver of patients with NAFLD. (B) The relationship between the area occupied by KCs estimated by image analysis and the RSE on super-paramagnetic iron oxide (SPIO)-MRI in patients with NAFLD. There was no correlation between these parameters (r=−0.252, p=0.287, n=20). (C) The relationship between the degree of hepatic steatosis and the area occupied by KCs in the livers of patients with NAFLD. No correlation between the degree of hepatic steatosis and the number of KCs was seen (r=−0.345, p=0.141, n=20).

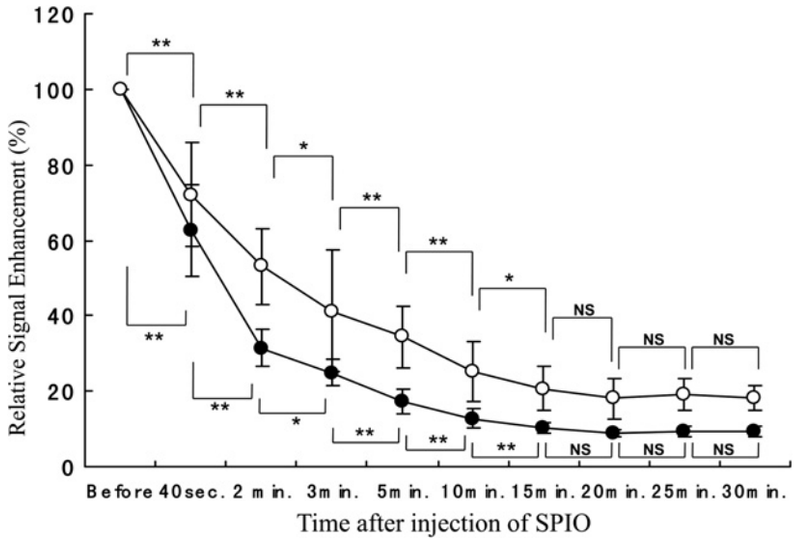

Figure 7 Changes in relative signal enhancement (RSE) in patients with non-alcoholic fatty liver disease (NAFLD) and chronic hepatitis C (CH-C) with time after injection of super-paramagnetic iron oxide (SPIO). RSE gradually decreased in both groups after injection of SPIO and had reached a plateau by 15 min (●, CH-C: n=10, ○, NAFLD, n=26, *p<0.05, **p<0.01).

DISCUSSION

In this study, using SPIO-MRI technology in experimental liver studies, we have shown conclusively that rats and patients with NAFLD have impaired KC uptake function. The importance of these findings lies in the fact that hyper-endotoxaemia may be implicated in the pathogenesis of NAFLD since KCs through their uptake properties provide the predominant protective barrier against the egress of endotoxin from the portal to the systemic circulation.[27] Reduced KC uptake function may, therefore, lead to higher endotoxin levels in the systemic circulation, as has been observed in patients with NAFLD and in animal models of NASH.[7 23 28] Given that overproduction of, and increased sensitivity to, cytokines such as tumour necrosis factor α and interleukin 1β from KCs[10 28] is also implicated in the pathogenesis of NAFLD, failure of KCs to clear endotoxin because of defective uptake function may further drive the production of these proinflammatory cytokines by KCs.

The impairment of KC uptake function was not due to a decrease in the number of KCs because these were raised both in experimental NASH livers compared with controls, and in patients with NAFLD compared with CH-C controls. In addition, KC uptake function as assessed by SPIO-MRI, in healthy volunteers was not different from that of patients with CH-C, but was different from that of patients with NAFLD. The reduced KC uptake function in patients with NAFLD, however, worsened with the degree of hepatic steatosis but, intriguingly though, was not related to the NAS. The mechanisms underlying this unexpected finding form part of ongoing studies in our group. We also compared the RSE on SPIO-MRI between the NASH (NAS ≥5; n=13) and non-NASH groups (NAS ≤4; n=7), and between the NASH and simple steatosis groups (NAS <4). We found no differences between the NASH group (21.04±6.79%) and non-NASH group (18.73±4.01%, p=0.485), nor between the NASH group (21.04±6.79%) and the simple steatosis group (18.53±4.45%, p=0.486).

Our animal data support previous studies that have shown defective KC uptake function in models of NASH.[9] In addition, Moriyasu *et al*[29] using ultrasonography showed reduced KC uptake function in patients with NASH. However, while ultrasonographic evaluation of KC function may be influenced by altered hepatic microcirculation, the SPIO-MRI methods described here have controlled for possible microcirculatory changes.

A possible criticism of our study is that we did not directly measure endotoxin levels in our patients with NAFLD and thus the reduced uptake function may not be of pathophysiological significance. However, if it is accepted that endotoxin is of importance in NAFLD and that KCs, as argued above, provide the main defensive barrier to endotoxin, then in the presence of defective KC uptake function, endotoxin levels would be expected to rise, as has indeed been shown.[6 7] The mechanism underlying the observed reduction in human KC uptake function remains to be investigated but may be related to defective leptin signalling, as previously described in models of NASH[9 30 31] or it may be related to saturation of uptake mechanisms by, for example, KC engulfment of apoptotic bodies or erythrocytes, as has been previously observed in NASH.[32 33]

In conclusion, we have shown using an SPIO-MRI technique that KC uptake function is defective in experimental NAFLD and in patients with NAFLD. This defective uptake function may be responsible for the observed raised levels of endotoxin that have previously been implicated in the pathogenesis of NAFLD.

Acknowledgements We are indebted to the technicians in the Department of Radiology, Kochi Medical School Hospital, for invaluable technical assistance with the SPIO-MRI studies.

Funding Grants-in-Aid for Scientific Research (C) 2006 Grant # 17590656, The Ministry of Education, Science, Sports and Culture, Japan; Wellcome Trust, UK (JAO).

Competing interests None.

Patient consent Obtained.

Provenance and peer review Not commissioned; externally peer reviewed.

REFERENCES

1. **Ioannou GN,** Boyko EJ, Lee SP. The prevalence and predictors of elevated serum aminotransferase activity in the United States in 1999–2002. *Am J Gastroenterol* 2006;**101**:76–82.
2. **James O,** Day C. Non-alcoholic steatohepatitis: another disease of affluence. *Lancet* 1999;**353**:1634–6.
3. **Ekstedt M,** Franzen LE, Mathiesen UL, *et al*. Long-term follow-up of patients with NAFLD and elevated liver enzymes. *Hepatology* 2006;**44**:865–73.
4. **Creely SJ,** McTernan PG, Kusminski CM, *et al*. Lipopolysaccharide activates an innate immune system response in human adipose tissue in obesity and type 2 diabetes. *Am J Physiol Endocrinol Metab* 2007;**292**:E740–7.
5. **Velayudham A,** Dolganiuc A, Ellis M, *et al*. VSL#3 probiotic treatment attenuates fibrosis without changes in steatohepatitis in a diet-induced nonalcoholic steatohepatitis model in mice. *Hepatology* 2009;**49**:989–97.

6. **Thuy S,** Ladurner R, Volynets V, *et al*. Nonalcoholic fatty liver disease in humans is associated with increased plasma endotoxin and plasminogen activator inhibitor 1 concentrations and with fructose intake. *J Nutr* 2008;**138**:1452—5.
7. **Ruiz AG,** Casafont F, Crespo J, *et al*. Lipopolysaccharide-binding protein plasma levels and liver TNF-alpha gene expression in obese patients: evidence for the potential role of endotoxin in the pathogenesis of non-alcoholic steatohepatitis. *Obes Surg* 2007;**17**:1374—80.
8. **Gao Y,** Song LX, Jiang MN, *et al*. Effects of traditional chinese medicine on endotoxin and its receptors in rats with non-alcoholic steatohepatitis. *Inflammation* 2008;**31**:121—32.
9. **Loffreda S,** Yang SQ, Lin HZ, *et al*. Leptin regulates proinflammatory immune responses. *FASEB J* 1998;**12**:57—65.
10. **Diehl AM.** Nonalcoholic steatosis and steatohepatitis IV. Nonalcoholic fatty liver disease abnormalities in macrophage function and cytokines. *Am J Physiol Gastrointest Liver Physiol* 2002;**282**:G1—5.
11. **Tilg H,** Diehl AM. Cytokines in alcoholic and nonalcoholic steatohepatitis. *N Engl J Med* 2000;**343**:1467—76.
12. **Fox ES,** Broitman SA, Thomas P. Bacterial endotoxins and the liver. *Lab Invest* 1990;**63**:733—41.
13. **Imai Y,** Murakami T, Yoshida S. Superparamagnetic iron oxide-enhanced magnetic resonance images of hepatocellular carcinoma: correlation with histological grading. *Hepatology* 2000;**32**:205—12.
14. **Ward J,** Guthrie JA, Scott DJ, *et al*. Hepatocellular carcinoma in the cirrhotic liver: double-contrast MR imaging for diagnosis. *Radiology* 2000;**216**:154—62.
15. **Elizondo G,** Weissleder R, Stark DD, *et al*. Hepatic cirrhosis and hepatitis: MR imaging enhanced with superparamagnetic iron oxide. *Radiology* 1990;**174**:797—801.
16. **Kato N,** Ihara S, Tsujimoto T, *et al*. Effect of resovist on rats with different severities of liver cirrhosis. *Invest Radiol* 2002;**37**:292—8.
17. **Tanimoto A,** Oshio K, Suematsu M, *et al*. Relaxation effects of clustered particles. *J Magn Reson Imaging* 2001;**14**:72—7.
18. **Hirose A,** Ono M, Saibara T, *et al*. Angiotensin II type 1 receptor blocker inhibits fibrosis in rat nonalcoholic steatohepatitis. *Hepatology* 2007;**45**:1375—81.
19. **Koteish A,** Diehl AM. Animal models of steatosis. *Semin Liver Dis* 2001;**21**:89—104.
20. **Lawaczeck R,** Bauer H, Frenzel T, *et al*. Magnetic iron oxide particles coated with carboxydextran for parenteral administration and liver contrasting. Pre-clinical profile of SH U555A. *Acta Radiol* 1997;**38**:584—97.
21. **Asanuma T,** Hirano Y, Yamamoto K, *et al*. MR imaging of hepatic injury in the LEC rat under a high magnetic field (7.05 T). *J Vet Med Sci* 1999;**61**:239—44.
22. **Asanuma T,** Ohkura K, Yamamoto T, *et al*. Three-dimensional magnetic resonance imaging of lung and liver tumors in mice by use of transversal multislice magnetic resonance images. *Comp Med* 2001;**51**:138—44.
23. **Bhunchet E,** Eishi Y, Wake K. Contribution of immune response to the hepatic fibrosis induced by porcine serum. *Hepatology* 1996;**23**:811—7.
24. **Park SH,** Kim PN, Kim KW, *et al*. Macrovesicular hepatic steatosis in living liver donors: use of CT for quantitative and qualitative assessment. *Radiology* 2006;**239**:105—12.
25. **Kleiner DE,** Brunt EM, Van Natta M, *et al*. Design and validation of a histological scoring system for nonalcoholic fatty liver disease. *Hepatology* 2005;**41**:1313—21.
26. **Ijaz S,** Yang W, Winslet MC, *et al*. Impairment of hepatic microcirculation in fatty liver. *Microcirculation* 2003;**10**:447—56.
27. **Farrell GC.** Is bacterial ash the flash that ignites NASH? *Gut* 2001;**48**:148—9.
28. **Solga SF,** Diehl AM. Non-alcoholic fatty liver disease: lumen-liver interactions and possible role for probiotics. *J Hepatol* 2003;**38**:681—7.
29. **Moriyasu F,** Iijima H, Tsuchiya K, *et al*. Diagnosis of NASH using delayed parenchymal imaging of contrast ultrasound. *Hepatol Res* 2005;**33**:97—9.
30. **Li Z,** Lin H, Yang S, *et al*. Murine leptin deficiency alters Kupffer cell production of cytokines that regulate the innate immune system. *Gastroenterology* 2002;**123**:1304—10.
31. **Yang SQ,** Lin HZ, Lane MD, *et al*. Obesity increases sensitivity to endotoxin liver injury: implications for the pathogenesis of steatohepatitis. *Proc Natl Acad Sci U S A* 1997;**94**:2557—62.
32. **Canbay A,** Feldstein AE, Higuchi H, *et al*. Kupffer cell engulfment of apoptotic bodies stimulates death ligand and cytokine expression. *Hepatology* 2003;**38**:1188—98.
33. **Otogawa K,** Kinoshita K, Fujii H, *et al*. Erythrophagocytosis by liver macrophages (Kupffer cells) promotes oxidative stress, inflammation, and fibrosis in a rabbit model of steatohepatitis: implications for the pathogenesis of human nonalcoholic steatohepatitis. *Am J pathol* 2007;**170**:967—80.